Specifics of the Molecular Conformations and Physicochemical Properties of Merocyanine Form of Spirooxazine Derivative: Insights from Experimental and Annealing-Molecular Dynamics Studies

Andreea Neacsu , Viorel Chihaia * , Valentin Alexiev , Georgi B. Hadjichristov , Minkovska Stela *

Posted Date: 7 January 2025

doi: 10.20944/preprints202501.0481.v1

Keywords: spirooxazines; merocyanine; solvatochromic properties; molecular dynamics; solvent polarity

Article

Specifics of the Molecular Conformations and Physicochemical Properties of Merocyanine Form of Spirooxazine Derivative: Insights from Experimental and Annealing-Molecular Dynamics Studies

Andreea Neacsu , Viorel Chihaia * , Valentin Alexiev , Georgi B. Hadjichristov , Minkovska Stela *

Posted Date: 7 January 2025

doi: 10.20944/preprints202501.0481.v1

Keywords: spirooxazines; merocyanine; solvatochromic properties; molecular dynamics; solvent polarity

Article

Specifics of the Molecular Conformations and Physicochemical Properties of Merocyanine Form of Spirooxazine Derivative: Insights from Experimental and Annealing-Molecular Dynamics Studies

Andreea Neacsu [1], Viorel Chihaia [1,*], Valentin Alexiev [2], Georgi B. Hadjichristov [3,4] and Stela Minkovska [2,4,*]

[1] Ilie Murgulescu Institute of Physical Chemistry, Romanian Academy, Spl. Independentei 202, 060021, Bucharest, Romania;

[2] Institute of Catalysis, Bulgarian Academy of Sciences, Acad. G. Bonchev Str., Bl. 11, BG-1113 Sofia, Bulgaria;

[3] Georgi Nadjakov Institute of Solid State Physics, Bulgarian Academy of Sciences, 72 Tzarigradsko Chaussee Blvd., BG-1784 Sofia, Bulgaria;

[4] "National Centre of Excellence Mechatronics and Clean Technologies", Kl. Ohridski Blvd, 8, Bl. 8, BG-1000 Sofia, Bulgaria.

* Correspondence: vchihaia@icf.ro (V.C.); stelamin@ic.bas.bg (S.M.)

Abstract: This research focuses on the merocyanine form of a new synthesized spiroindolinonaphthoxazine compound. The merocyanine molecule (abbreviated as MC) has multiple fragments with different degrees of mobility. The conformational changes and the flexibility of MC in presence and in absence of the solvent molecules were studied by Annealing-Molecular Dynamics cycles, providing insights into how they orient and interact with each other and with solvent molecules. The molecular packing of MC in presence and in absence of solvents with different polarities was thoroughly investigated in order to determine, how the physicochemical interactions with the solvent influence the structure and stability of the MC molecule. Furthermore, the powders of MC obtained from its solutions in water, methanol, ethanol and acetonitrile were experimentally characterized using differential scanning calorimetry, thermogravimetry, Fourier transform infrared spectroscopy, and scanning electron microscopy. Both calculations and experimental results reveal the effect of the solvent polarity on the dissolved MC molecule.

Keywords: spirooxazines; merocyanine; solvatochromic properties; molecular dynamics; solvent polarity

1. Introduction

The color-changing phenomenon is usually related to an energy source such as an external or internal stimulus. Chromogenic materials exhibit various types of chromism, such as photochromism, electrochromism, thermochromism, mechanochromism, solvatochromism, chemochromism, and biochromism, depending on the nature of the stimulus [1]. Solvatochromism refers to the phenomenon where the color of a compound changes when dissolved in different solvents. Solvatochromism can be used to sense small concentrations of polar molecules in a non-polar system, to detect explosives [2], as well as to evaluate certain solvent parameters to assess solubility phenomena and predict suitable solvents for particular applications [3]. A water-molecule- or humidity-responsive system, called a hydrochromic material, is also used as functional inks and textile colorants in industrial systems [4]. In particular, the solvatochromic properties of merocyanine

 doi:10.20944/preprints202501.0481.v1

compounds make them valuable as polarity indicators for studying solvent effects on molecular structure [5].

In this work the target compound is the merocyanine form (see Figure 1a) of a spiroindolinonaphthoxazine derivative with the corresponding IUPAC name 4-[(2E)-1,1-dimethyl-2-({[(1Z)-2-oxo-1,2-dihydronaphthalen-1-ylidene]amino}methylidene)-1H,2H,3H-benzo[e]indol-3-yl]butane-1-sulfonic, abbreviated here as MC. The investigated MC molecule is a new synthetized product by us, exhibiting photochromic and solvatochromic properties [6]. The bond-twisting mechanism involves the conversion of closed form of the *spiro*-molecule to merocyanine (open form) through a series of steps. Upon excitation by UV light, the closed form molecule undergoes a reaction where the C_{spiro}–O bond is broken to form the colored MC isomer. This process involves the elongation of the C_{spiro}–O distance to reach the cis-MC structure, followed by rotation around the central torsion angle to transition to the trans-MC structure [7,8]. C_{spiro} denotes the rigid *spiro* carbon that connects the indoline moiety and the central oxazine ring. The interconversion between these two forms can be triggered by various factors such as light, heat, or the presence of specific metal ions [9,10]. The conversion from closed form to open form (MC) under UV light irradiation and different metallic ions was already discussed in our previous works [6,8].

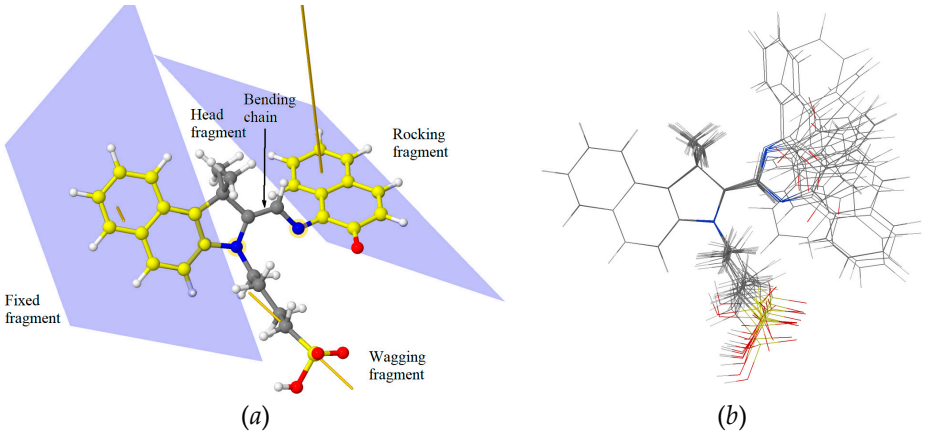

Figure 1. The MC functional regions (a) and various stable isomers with the superposed fragment $C_{10}NH_6$ (b). The carbon atoms of the two fragments $C_{10}NH_6$ are indicated by yellow color; the average planes that contain them are indicated, together with the corresponding normal vectors. The direction of the wagging tail is indicated by the yellow line. The colors of balls indicate the type of the respective atoms: green and gray balls - carbon, red - oxygen, blue - nitrogen, and withe - hydrogen).

We attempted to use several solvents to obtain a crystalline system, but these efforts were unsuccessful. This prompted us to investigate the effects of solvents on the MC system. Indeed, the MC compound studied here is sensitive to its environment, and solvent interactions can induce changes in the MC molecular conformations, resulting in different polymorphic forms. The phenomenon of solvatochromism in spirooxazines is associated with variations in solute-solvent interactions across solvents with different polarities. The solvatochromic behavior of MC can be explained by considering the variation in geometry induced by the solvent and the stabilization of energy levels introduced through solvation [11]. The MC compound showed solvatochromic properties with solvents water, acetonitrile, ethanol and methanol. The chosen solvents have a different number of OH groups, with characteristic solvent-solvent hydrogen bonds topology and different availability/ability to form hydrogen bonds with the solvated MC molecules that might control the MC folding and stability. The evaporation of solvent allows the compound to adopt a specific molecular arrangement based on the solvent's influence during the transition to a solid state [12,13].

To our knowledge, no theoretical or experimental investigations have been conducted on MC molecules and MC-solvent systems, aside from our own characterizations [6,8]. Thus, this article presents the initial stage of the experimental and computational characterization of solid-phase MC

 doi:10.20944/preprints202501.0481.v1

properties. We experimentally examined the molecular structure and thermal properties of MC polymorph powders obtained after solvent evaporation using differential scanning calorimetry (DSC), thermogravimetry (TG), attenuated total reflectance Fourier transform infrared spectroscopy (ATR-FTIR), and scanning electron microscopy (SEM). To gain deeper insights into the effects of these solvents, we decided to complement the experimental study with atomistic calculations. The conformational changes and flexibility of MCs in the presence and absence of solvent molecules are investigated by Annealing-Molecular Dynamics (MD). This approach allowed us to better understand the solvent-induced effects on the properties of MC in the solid phase and the challenges associated with obtaining crystalline MC. The studied MC molecule is characterized by a triple-fragment branched topology, and we proposed an analysis scheme based on this topology in order to characterize the flexibility and the packing of the molecules. This study provides insight into how MC molecules orient and interact with each other and with solvent molecules. The obtained results are useful for tuning and designing new photochromic molecules for different specific application. The solvatochromism of these compounds makes them interesting for practical application. Controlling molecular switching opens the door to new opportunities on fundamental and applied materials science.

2. Materials and Methods

2.1. Computational Details

The MC molecule with an asymmetric triskelion topology presents several functional regions (see Figure 1a). The central pentagonal ring C_4N, part of the *spiro* group, serves as a connector for various parts of the molecule. Two $C_{10}NH_6$ groups are observed. One group is completed by a carbon atom that belongs together with its own nitrogen to the pentagonal ring C_4N. The fragment $C_{11}NH_6$ shares one C and one N with the pentagonal ring, which makes them a rigid fragment. Therefore, we call the fragment $C_{11}NH_6$ as fixed. It will give the orientation of the MC molecule. The second group is completed by an oxygen atom. The fragment $C_{10}NOH_6$ is mobile as its nitrogen atom is connected by a CH_2 group to the nitrogen atom from the pentagonal ring C_4N. The $C_{10}NOH_6$ is called rocking fragment, as it is highly mobile (see Figure 1b) due to the flexibility of the C-CH_2-N chain (called bending chain). Three dihedral angles define the spatial arrangement of the MC conformers. Another important fragment, called wagging due its high flexibility, is the butyl-1-sulfonate chain $(CH_2)_4$–SO_3H that is connected to the nitrogen atom of the pentagonal ring C_4N and ends with the sulfonyl group SO_3H. The five dihedral angles defined by the N and C skeleton atoms give the chain shape and the orientation of the wagging fragment $(CH_2)_4$–SO_3H. The C–S bond defines the orientation of the wagging fragment. The central pentagonal ring together with the two methyl groups CH_3 connected to one of its carbon atoms form the head fragment. The head fragment moves solitarily with the fixed fragment $C_{11}NH_6$.

The MC molecule, with the chemical formula $C_{29}H_{28}N_2O_4S$, contains 64 atoms being already at the limit of applicability of the Ab Initio electronic structure methods, making these methods prohibited for the study of the solvation effects on the MC molecule. Due to the large number of the freedom degrees even the semiempirical methods are not applicable for such studies. The application of the empirical force fields are recommended, but the study of the MC solvation for several solvents limit the applicability of long Molecular Dynamics or Monte Carlo simulations. Therefore, in the present study we performed geometry optimization of the stereometric configuration of MC molecule using the empirical force field COMPASS (Condensed-phase Optimized Molecular Potentials for Atomistic Simulation Studies) [14] implemented in the simulation package *LAMMPS* [15]. COMPASS force field, designed for lattice energy calculations on general organic molecular crystals, gives very good results for gas, liquid and solid systems [16]. For the visualization of the molecular systems the software *jmol* was used [17].

The most stable isomers of the isolated MC molecule, determined by COMPASS geometry optimization for fixed dihedral angles along the bending chain of MC molecules, are presented in

 doi:10.20944/preprints202501.0481.v1

Figure 1b. We can see that indeed the fixed fragment is almost rigid, and that the rocking fragment reorients depending on the dihedral angles along the bending chain. The solvent could influence the stability of the MC molecule, with a preference for one isomer over another. The two isomers mentioned in the Introduction, cis-MC and trans-MC, are the most stable pristine conformer (see Figure S1c,d, respectively, in the Supplementary Materials). The trans-MC isomer is more stable than the cis-MC, with 3.9 and 2.7 kcal/mol as predicted by the COMPASS-FF and DFT methods, respectively (see Table S1). However, other two configurations that involve the wagging fragment folding such that the terminal OH group of the sulfonic acid SO_3H forms a hydrogen bond with the oxygen or nitrogen atom of the bending chain ring, as shown in Figure S1a,b in Supplementary Materials. The formation of hydrogen bonds by the OH group with the oxygen atom from the opened ring is more energetically favored (with 3.7 and 3.0 kcal/mol, as predicted by the COMPASS-FF and DFT methods, respectively). In this arrangement, the stability surpasses that of the trans-MC isomer by 12.5 and 4.3 kcal/mol, as predicted by the COMPASS-FF and DFT methods, respectively. The DFT calculation are done with the code *orca*,[18] using the hybrid exchange-correlation functional B3LYP [19] and the basis set 6-31+G(d,p) [20] in the spin unrestricted approach. The COMPASS force field reproduce the order of the stable MC isomers predicted by the DFT calculations.

The solvation was simulated by randomly packing 10 cis-MC molecules together with 100 solvent molecules X = A (acetonitrile), E (ethanol), M (methanol), and W (water), producing 7500 configurations for each solvated system. Since the cis-MC isomer is the stable isomer following the oxazine ring opening during the transition from the spiroindolinonaphthoxazine to merocyanine form, we have selected it as reference. The high computational effort due to the high number of freedom degrees limited us to moderate size systems, but large enough to have an accurate statistics, relevant for many possible isomers of MC molecule. The 100 solvent molecules assure a good mobility of the MC molecules, with sufficient number solvent molecules to properly surround each of the MC molecule. The high concentration of MC molecules correspond to MC-solvated systems closed to desolvation state. In order to let the molecules to adjust their positions and orientations based on their interactions the initial system has a low density 0.6 g/cm^3 comparing with that characteristic to each mixture (around 1.2 g/cm^3). The obtained systems were fully optimized, considering the fractional coordinates of atoms and the simulation box parameters.

The most stable 10 configurations of each solvated system characterized by lowest COMPASS3 potential energy were further equilibrated by isothermal–isobaric ensemble (NPT - constant number of particles N, pressure P and temperature T) MD simulations of 5 ns, with a time step of 1.0 fs. The temperature of 300 K was controlled by Nose-Hoover thermostat (Q_{ratio}=0.01), and the value of the pressure (0 bar) by Berendsen barostat. The temperature and total energy converges to equilibrium values during the MD calculations and therefore, the MC – solvent packing is considered to be achieved. In order to see how the solvent affects the structure of dry systems we prepared them by elimination of one solvent molecule at each 100 time steps during of 20 ps of NPT MD simulations for each MC-solvated system. We use a short notation MCX and MC(X) for the solvated and desolvated MC molecules, respectively, where the solvent molecules are denoted as X = A, E, M and W.

The final configurations of solvated MCX and desolvated MC(X) were further optimized by full static calculations, for the fractional coordinates of the atoms, as well as for the size of lattice edges and for the lattice angles. The configuration characterized by the lowest potential energy was selected for further relaxations by annealing for ten Molecular Dynamics cycles, each cycle being followed by an accurate optimization step. The initial and maximum temperatures were 300 and 500 K, respectively and the pressure was set to 0 bar. Each NPT cycle consisted in 50000 time steps of 1.0 fs each.

The most stable configurations of the ten optimized solvated MCX and desolvated MC(X) systems are characterized by analysis of the orientation of the fixed, rocking and wagging fragments, center-center distances of the MC molecules, the intra- and intermolecular hydrogen bonds formed by the MC molecules. The orientation of the fixed and rocking fragments are defined by the normal

 doi:10.20944/preprints202501.0481.v1

vectors to the best-fit plane of the two hexagonal rings formed by the carbon atoms, and the orientation of the wagging fragment is defined by the C-S direction of the group C-SO_3H. The angles between the different analyzed vectors have values between 0 and 90 degrees, being measured as shorter angles formed by the support directions of two vectors.

The formation energy of the compound $MC{-}X$ = MCX or MC(X) per MC molecule, with X= acetonitrile, ethanol, methanol and water, is determined via the following equation

$$E_{form} = \left(E\left(MC{-}X\right) - n_{MC}E(MC) - n_X E(X)\right)/n_{MC}$$

where $E(MC{-}X)$, $E(MC)$ and $E(X)$ are energies of the system MC-X, MC molecule in the cis- state and the solvent molecule X, respectively. $n_{MC} = 10$ specifies the number of MC molecules and $n_X = 100$ or 0 is the number of X molecules in the solvated or desolvated system MC-X, respectively. The cis-MC isomer was selected as reference for the MC molecule.

2.2. Experimental

2.2.1. Materials

The synthesis of the spirooxazine compound and its physico-chemical properties related to photochromism, as well as its MC form were described elsewhere [6,8]. The purity of the material that was used in this study both for the analysis in solid state and in the formulation of the solutions was identified as having a purity value of 99%. The fresh synthetized dark-blue powder was used in different preparation at room temperature (25 °C ± 2 °C). In this study, MC of concentration 10^{-4} M in different solvents was used for preparation of the desolvated powders. Solvents used in sample preparation were acetonitrile (A), deionized double distilled water (W), ethanol (E) and methanol (M). Different forms of MC were obtained by isothermal evaporation in vacuum of the solvents and the resulted powders were further analyzed by different methods.

2.2.2. Methods

Thermogravimetric data (TG/dTG) and also DSC curves of MC powders was obtained using Setaram Setsys Evolution 17 with open alumina crucibles of 100 µL volume. The calorimeter was calibrated using recommended standards of indium (ΔH_{fus} = 28.46 J/g). The calorimeter was operated at a heating rate of 10 °C/min in the temperature range from 20 °C to 600 °C. The sample mass have been 1.13 mg and was scanned in flowing argon atmosphere (16 mL/min). The relative uncertainty of the measurement was ±0.15%.

Fourier transform infrared (FT-IR) spectra of the samples were recorded at room temperature by Nicolet iS10 FT-IR spectrometer covering the range from 4000 to 600 cm^{-1}. The spectra were acquired with an average of 32 scans, with spectral resolution of 4 cm^{-1}, in attenuated total reflectance (ATR) mode.

The morphology of the samples were investigated by scanning electron microscopy (SEM) using a high-resolution microscope, FEI Quanta 3D FEG, operating at 15kV, in low vacuum mode with Low Vac Secondary Electron Detector (LVSED). The material understudy was positioned on a double-sided carbon tape, without coating.

3. Results

3.1. The Conformational Analysis

The stability, stereometric configuration and packing of the MC molecules are influenced by various interactions, including the electrostatic, hydrogen bonding, aromatic π-stacking, and hydrophobic and hydrophilic interactions with the neighboring MC and solvent molecules. The $C_{10}NH_6$ groups in both the fixed and rocking segments of the MC molecules minimize their contact with the OH- groups of the solvent molecules, significantly affecting the packing of the MC

 doi:10.20944/preprints202501.0481.v1

molecules. Additionally, the flexible wagging and rocking fragments can adjust their orientations to enhance their interactions with adjacent MC and solvent molecules.

The fully optimized configurations of MC molecules obtained by COMPASS3 force field optimization, for the solvated and desolvated systems, are shown in Figure 2. The distribution of angles formed by normal vectors to the average planes that containing the fixed and rocking fragments of MC molecules in acetonitrile (see Figure S2 in Supplementary Materials) reveals two preferred orientations for the rocking fragment relatively to the fixed fragment, centered to θ = 50° and 75°, respectively. Upon desolvation, the orientation of the rocking fragments changes significantly, favoring the configurations with lower angles. For the MCE system, the orientations are similar to those in the MCA system, though desolvationleads to two configurations where the rocking fragments are nearly perpendicular to the fixed fragments. In the MCM case, the configurations predominantly exhibit angles θ clustered around 45°, with a spread between 20° and 90° after desolvation. In contrast, when solvated in water, the MC molecules show a nearly constant distribution of angles between 30° and 90°. Very similar configurations are observed in the desolvated MC(W) system.

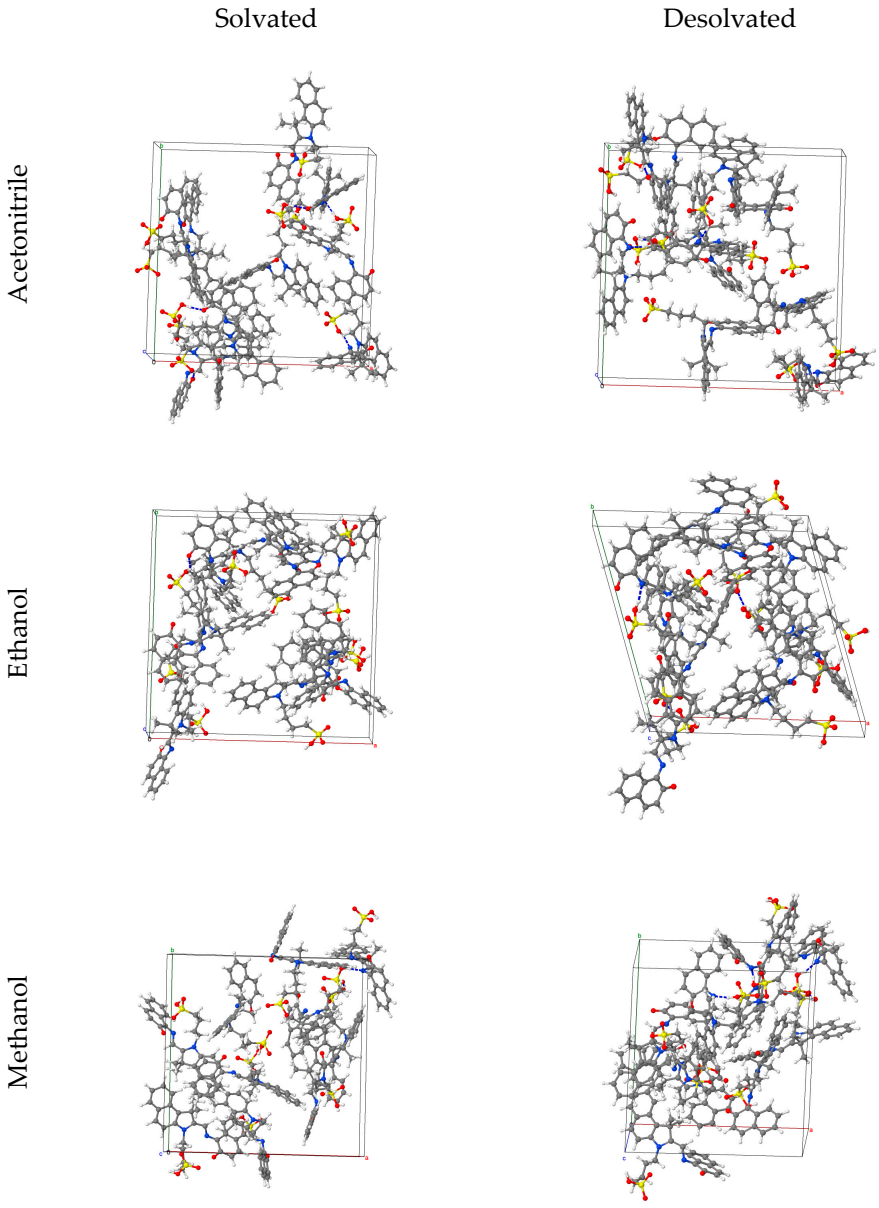

 doi:10.20944/preprints202501.0481.v1

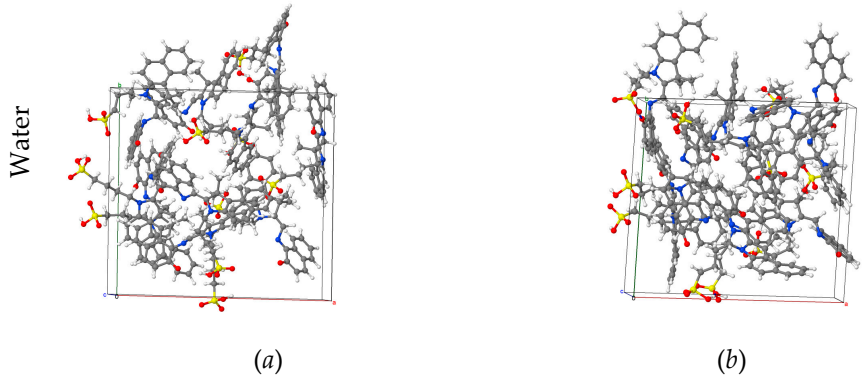

Figure 2. The configurations of the most stable MC system solvated (a) and desolvated (b) for several solvents: acetonitrile, ethanol, methanol and water. For a better visibility, the molecules of solvents are not shown for the solvated systems. The blue dashed lines indicate the intra-molecular hydrogen bonds.

The distributions of angles formed by normal vectors to the average plane that contain the fixed fragment and the orientation vector of the wagging fragment of the MC molecules for solvated and desolvated systems show that the wagging fragments are very flexible being characterized by an almost a continuous angular distribution with higher probability for a perpendicular orientation to the fixed fragment (see Figure S3 in Supplementary Materials). The desolvated systems are characterized by a larger amount of MC molecules with larger angles.

The distributions of angle formed by normal vectors to the average plane containing the rocking fragment and the orientation vector of the wagging fragment of the MC molecules solvated in acetonitrile are nearly uniform regarding the relative orientation of the two fragments (see Figure S4-MCA in Supplementary Materials). In the desolvated system MC(A) , the wagging fragment shows a preference for orientations corresponding to angles in the middle interval. For the solvated MC in ethanol, the angle distribution is concentrated between 30° and 60°, with a notable peak around 60°. There are also a few smaller peaks outside this range. For the desolved system MC(E), distinct peaks at 20 and 80 degrees, along with notable occurrences in the 50 to 60 degrees. The graphs for MCM and MC(M)) emphasize angles between 40° and 80°, with MCM favoring 60° and the MC(M) favoring 20°. The relative orientations of the rocking and wagging fragments of MC solvated in water MCW and desolvated one MC(W) show more discrete distributions compared to the other systems. However the MCM system still highlights angles around 60°, while the MC(W) favors 20°, with a more consistent spread across the mid-range angles.

The analyses of the densities of the equilibrated solvated systems reveal an ordering that corresponds to the polarity of the solvents: MCA < MCE < MCM < MCW. Upon desolvation, the densities are increase but differ for the same solid MC material: MC(E) < MC(A) < MC(W) < MC(M), reflecting variations in the molecular packing of MC. The shortest distances between the mass centers of two MC molecules were found to be 5.13, 5.73, 6.47 and 7.14 Å for solvated MC molecules in methanol, acetonitrile, water and ethanol MCM < MCA < MCW < MCE (see Table 1). The order changes for the desolvated MC systems, where the inter-MC distances are 4.74 Å, 5.47 Å, 6.37 Å and 7.15 Å, following the sequence MC(M) < MC(A) < MC(E) < MC(W). While a reduction in inter-MC distances was expected upon solvent removal, an increase was observed for MC(W). The distribution of the inter-MC distances for the solvated systems (see Figure S5 in Supplementary Materials) show less dispersion for MCW and a greater dispersion for MCM, reflecting more clustered and dispersed MC-based systems, respectively. This trend persist in the desolvated systems. Despite the increase of the shortest inter-MC distance for MC(W), a shift towards lower inter-MC distances indicates a compaction of the MC molecules upon desolvation.

 doi:10.20944/preprints202501.0481.v1

Table 1. The minimum distance between the MC fragments centers (d_{min}), the simulation cell and free volume, and the formation energy that are obtained by COMPASS force field annealing optimizations, for solvated MCX and desolvated MC(X) molecules, where X=A, E, M, W denotes the type of solvent molecules.

Solvent	State	d_{min} [Å]	Density [g/cm³]	Box Volume [Å³]	Free Volume [Å³]	Formation Energy per MC Molecule [kcal/mol]
Acetonitrile	MCA	5.73	1.110	13622.4	0.0	-164.8
	MC(A)	5.47	1.226	6671.7	1.1	-51.8
Ethanol	MCE	7.14	1.126	14173.1	3.9	-164.4
	MC(E)	6.37	1.211	6443.6	62.3	-53.0
Methanol	MCM	5.13	1.142	11938.2	0.3	-57.2
	MC(M)	4.74	1.290	6566.8	1.8	-53.2
Water	MCW	6.47	1.203	9394.1	1.1	-56.3
	MC(W)	7.15	1.281	6486.7	5.1	-44.2

The density and the volume of the simulation box are not particularly informative in this context since the solvent molecules have themselves different sizes. Instead, we characterized the packing of MC molecules by examining the unoccupied space available near the MC molecules, known as **solvent surface free volume, which reflects the** potential interaction space for solvent molecules around the MC molecules. In the case of MCA, no free space is available for solvents, and only a very small space in the case of MCM. However, MCE and MCW show some empty spaces, particularly near the $C_{10}NH_6$ groups of the fixed and rocking fragments of MC molecules, which repeal the OH-groups from ethanol and water. Analyzing the systems, we observe that the methanol molecules do not disperse between the MC molecules, but instead accumulate in the pockets formed by the MC molecules. The system remained after the methanol removal from the simulation box is the most stable desolvated system, being characterized by the lowest formation energy (see Table 1).

The nitrogen and oxygen atoms in the central region of the MC molecule can form intramolecular hydrogen bonds with the hydrogen atom of the sulfonyl group through bending of the wagging fragment within the same molecule (see Figure 3a,b) or from another MC molecule (see Figure 3b). Additionally, these central nitrogen and oxygen atoms, along with the oxygen and hydrogen atoms of the sulfonyl group, can form intermolecular hydrogen bonds with the OH groups of the solvent molecules. In contrast, the fixed and rocking fragments are hydrophobic, tending to repel the OH groups of the solvent. Table 2 presents the number of the intra-MC and inter-MC hydrogen bonds, as well those formed with the solvent molecules. It is noted that, except for methanol, where the number of the hydrogen bonds between MC molecules remain unchanged, the number of hydrogen increases after desolvationin all other cases. The system MC(M) is characterized by a high number of intramolecular hydrogen bonds (see Table 2) that are specific to MC-HB_O, the most stable isomer of MC. Thus, the highest stability of MC(M) comparing to other desolvated systems MC(X) can be justified.

Table 2. The number of hydrogen bonds formed between different molecules for solvated MCX and desolvated MC(X) systems, where X=A, E, M, W denotes the type of solvent molecules..

Solvent (Solv)	State	Hydrogen Bonds (Donor→Acceptor)				
		Intra-MC	Inter-MC	MC→Solv	Solv→MC	Solv→Solv
Acetonitrile	MCA	2	7	0	0	0
	MC(A)	0	15	-	-	-
Ethanol	MCE	0	2	0	29	69
	MC(E)	0	10	-	-	-
Methanol	MCM	0	4	0	28	76
	MC(M)	8	4	-	-	-
Water	MCW	0	2	0	69	173

 doi:10.20944/preprints202501.0481.v1

MC(W)	1	11	-	-	-

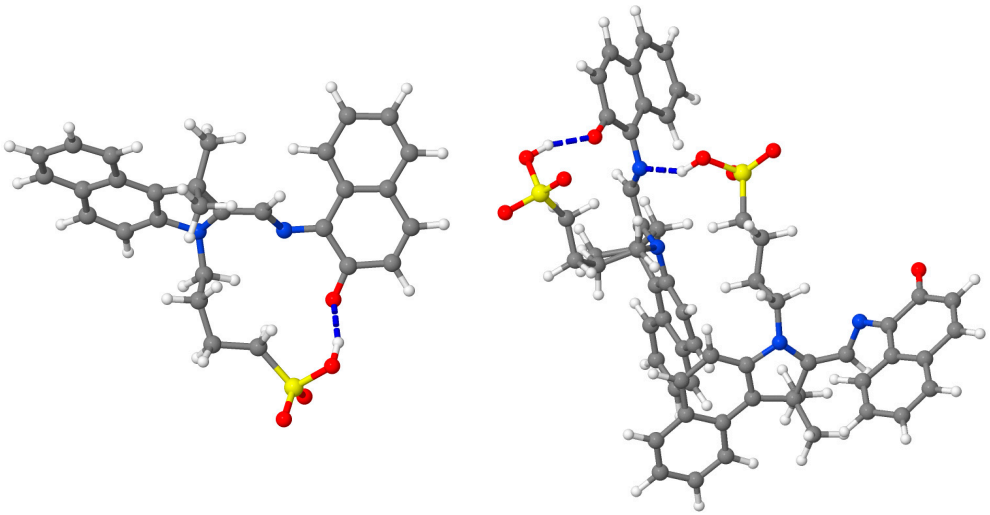

(*a*) (*b*)

Figure 3. Examples of the intramolecular (*a*,*b*) and intermolecular (*b*) hydrogen bonds formed by the MC molecules solvated in acetonitrile (MCA system). The hydrogen bonds are indicated by blue dashed lines. The representation of the atoms is the same as in Figure 1.

The distributions of angles formed by normal vectors to the average planes containing the fixed fragments of neighboring MC molecules show similar fairly uniform spread across angles, with a few prominent peaks. This suggests a similar distribution pattern in angle preference, though slight variations in intensity and slight shifts between the solvated and desolvated systems (see Figure S6 in Supplementary Materials). Distinct features associated with the orthogonal arrangement of two neighboring fixed fragments are evident in both solvated and desolvated systems. The presence of very low angles suggests the stacking of MC molecules with the same orientation of the fixed fragments.

The rocking fragments of neighboring MC molecules in acetonitrile exhibit an angle distribution between 0° and 90°, with notable peaks at approximately 20°, 50°, and 80° (see Figure S7 in Supplementary Materials). The peak near 80° is the highest, followed by the one around 50°. In the desolved MC(A) the rocking fragments show similar arrangements, with minor variations in intensity, indicating comparable trends between MCA and MC(A). The other solvated and desolvated systems display similar trends in rocking-rocking angle distribution, with peaks generally occurring around 30°, 50°, and 80°, with 80° being consistently being the dominant peak. This suggest that the relative arrangements of the rocking fragments are largely similar across systems, with only slight differences in peak heights and intensities.

The wagging fragments of neighboring MC molecules, both in solvated and desolvated systems exhibit similar angle distribution patterns within specific ranges, particularly around 40° and 70° (see Figure S8 in Supplementary Materials). However, there are subtle variations in intensity and distribution between the graphs. In general, the solvated MC samples show a broader distribution with multiple smaller peaks across various angles, while the desolvated samples tend to have angle distributions shifted slightly towards lower angles. This behavior highlights the notable flexibility of the wagging fragments.

3.2. FT-IR Analysis

In Figure 4a it can be seen the naked-eye pictures and the color of the studied MC desolvated powders. The FTIR - ATR spectra of these powders are presented in Figure 4b and the observed vibrational frequencies of the desolvated samples are listed in Table 3. From left to right in Figure 4a,

 doi:10.20944/preprints202501.0481.v1

the colors of the powders range from navy to green to dark red, corresponding to the increasing polarity of the solvent. Thus, the chromatic shift in the MC polymorphs is attributed to the polarity of the solvent through solute-solvent interactions, resulting in changes such as shifts in the vibrational frequencies of certain functional groups due to modifications of bond angles and dihedral angles between atoms within the MC. By comparing the FTIR spectra of the obtained MC isomers, insignificant differences were observed for MC(A), MC(E), and MC(M), while some differences are evident for MC(W). Water provides a medium with increased hydrogen bonding capabilities; thus, the stronger interaction between water molecules and MC may result in more pronounced changes in the FTIR spectrum compared to when the molecule is in a less polar solvent environment.

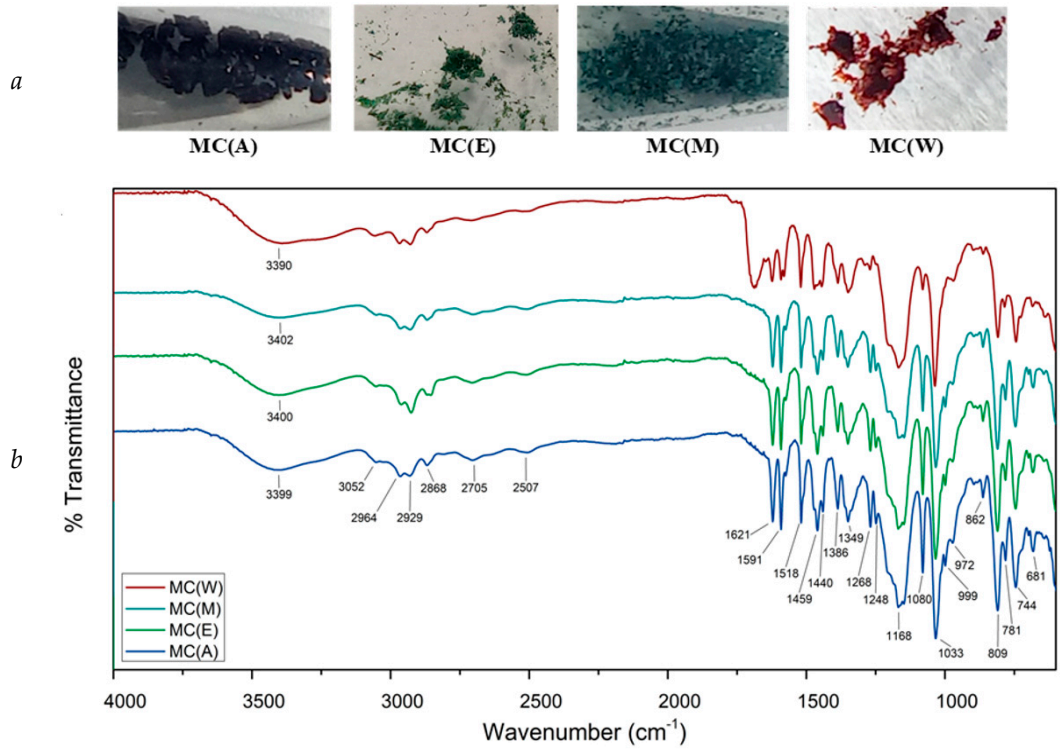

Figure 4. (*a*) - Photographs showing the naked-eye color of MC desolvated powders from acetonitrile – MC(A), ethanol – MC(E), methanol – MC(M) and water – MC(W). ***(b)*** **-** ATR FT-IR spectra for merocyanine forms MC(A), MC(E), MC(M) and MC(W).

Table 3. Assignment of the ATR-FTIR peaks for MC polymorphs.

MC(A)	MC(E)	MC(M)	MC(W)	Band Assignment
3399	3400	3402	3400	O-H bending vibrations mode of H-O-H
3052	3052	3051	3055	C–H stretching of the methylene group; (sp^2, stretch)
2964	2961	2964	2967	C–H stretching of the methyl group; (sp^3, stretch)
2929	2925	2929	2929	C–H stretching of the methylene group; (sp^2, stretch)
2868	2854	2868	2869	C–H stretching of the methyl group; (sp^3, stretch)
2705	2706	2702	2709	(CO)-H stretch
2507	2506	2507	-	C-O stretching in presence of H-O-H
-	-	-	2524	C-O stretching in presence of H-O-H
1769	1769	1769	1765	C=O stretching - oxygen atom conjugated with aromatic
-	-	-	1688	C=O stretch for conjugation with aromatic double bond
-	-	-	1646	C=O bending mode in presence of H-O-H
1621	1621	1621	1623	C=O in quinone structure; amide I

 doi:10.20944/preprints202501.0481.v1

1591	1591	1591	1591	-C=N- in open-chain imino; C=C in aromatic structure
1574	1574	1574	1580	C=N in aromatic structure
1518	1518	1519	1520	C=N vibrations in presence of CO
1459	1459	1459	1471	C=N vibrations; C-C in aromatic structure
1440	1440	1440	1445	C=N trans aromatic; C=C in aromatic structure; CH bend
1386	1386	1386	1386	C-H in gem-dimethyl
1349	1350	1350	1349	C-N stretching vibration
-	-	-	1288	C-N stretching vibration
1268	1269	1269	1270	C-O deformation vibration in presence of -SO_3-
1248	1249	1248	1249	S-O stretching deformation in presence of C-O
1168	1168	1168	1168	C-O stretching combined with CH_3 rocking vibration
1148	1148	1148	1148	S=O stretching in C-SO_2-OH
1080	1080	1080	1080	-SO_3- sulfonate ion
1033	1033	1033	1036	S=O symmetric stretching in sulfonate
999	999	999	-	CH_3 rocking vibration; -CH_2- group
972	972	972	969	C-O stretching and C-N stretching vibrations
862	863	862	862	C-O stretching; cyclohexene derivative
809	810	810	809	aromatic C-H out-of-plane bending, -CH_2- rocking
781	781	781	785	C-H out-of-plane; polynuclear aromatic compounds
744	745	745	743	C-C in aromatic compounds; C-N in ring
681	682	681	684	C-S stretching vibration in CH_2-S-, C-H bending

For the studied samples, the associated frequencies of (C-O)*spiro* structure appear in the spectra shifted to lower wavenumbers than usual (969 cm^{-1} for MC(W) and 972 cm^{-1} for the other MC samples), which means a lengthen of C-O bond in *spiro* structure [21]. After the ring-opening process the spatial orientation of the butyl sulfonic moiety shown by the position of the peaks ascribed to the hydrocarbon chain, (in Table 3) was affected especially for MC(W). As shown in Figure 4, the wide characteristic band in the range of 3700 cm^{-1} to 3100 cm^{-1} (including 3399 cm^{-1}, 3390 cm^{-1}, 3400 cm^{-1} and 3402 cm^{-1} for MC(A), MC(W), MC(E) and MC(M) respectively) could be attributed to the –OH stretching vibration due to -SO_3H group and of the physical adsorption of water [22].

The characteristic band at 1646 cm^{-1} only for MC(W) could be attributed to the stretching vibration of water when hydrogen bond is present. The typical band related to C=O (carbonyl stretching vibration) at 1769 cm^{-1} in MC(A), MC(E), MC(M) appear at a relatively high frequency in the IR spectra while for MC(W) sample, the carboxyl group appears at lower frequency in IR spectrum (1765 cm^{-1}). This shift occurs due to the resonance effects between the C=C or phenyl group and the C=O group, which affects the bond strength and frequency of vibration. Only in MC(W) spectrum, the pre-eminent peak at 1688 cm^{-1} and the other two faint peaks (~1765 cm^{-1} and 1646 cm^{-1}) indicating the occurrence of intermolecular hydrogen bonds with a combination of phenomena related to presence of bonded water molecules [23]. The peak at 1646 cm^{-1} in MC(W) typically could be attributed to the stretching vibration of water when hydrogen bond is present. The specific interpretation may be related to the presence of the oxygen atom in the carbonyl group that can act as a hydrogen bond acceptor, forming hydrogen bonds with hydrogen atoms attached to electronegative atoms like oxygen or nitrogen [24,25].

In the range of 1750 cm^{-1} to 1650 cm^{-1} the spectra of the MC(A), MC(E), MC(M) isomers present a small broad peak which arise from vibrations involving multiple bonds or a complex molecular structure caused by a possible remain solvent. The group of three separated bands at 1621 cm^{-1} (1623 cm^{-1} in MC(W)), 1591 cm^{-1} and the shoulder at 1574 cm^{-1} (1580 cm^{-1} in MC(W) are related to C=N bond and indicate that the nitrogen in the MC molecules is interacting with solute molecules [22,26].

Preprints.org (www.preprints.org) | NOT PEER-REVIEWED | Posted: 7 January 2025 doi:10.20944/preprints202501.0481.v1

Moreover, the presence of amide I bands (peaks at about 1621 cm^{-1} and 1623 cm^{-1}) suggest the possibility of hydrogen bonds and a possible twist of naphtho-moiety of the MC molecule.

3.3. DSC/TG Thermal Analysis

Figure 5 shows the thermal analysis results for the solid powders of the MC samples, obtained by desolvationfrom different solvents. The thermogravimetric parameters determined from the analysis of the thermogravimetric curves are presented in Table 4.

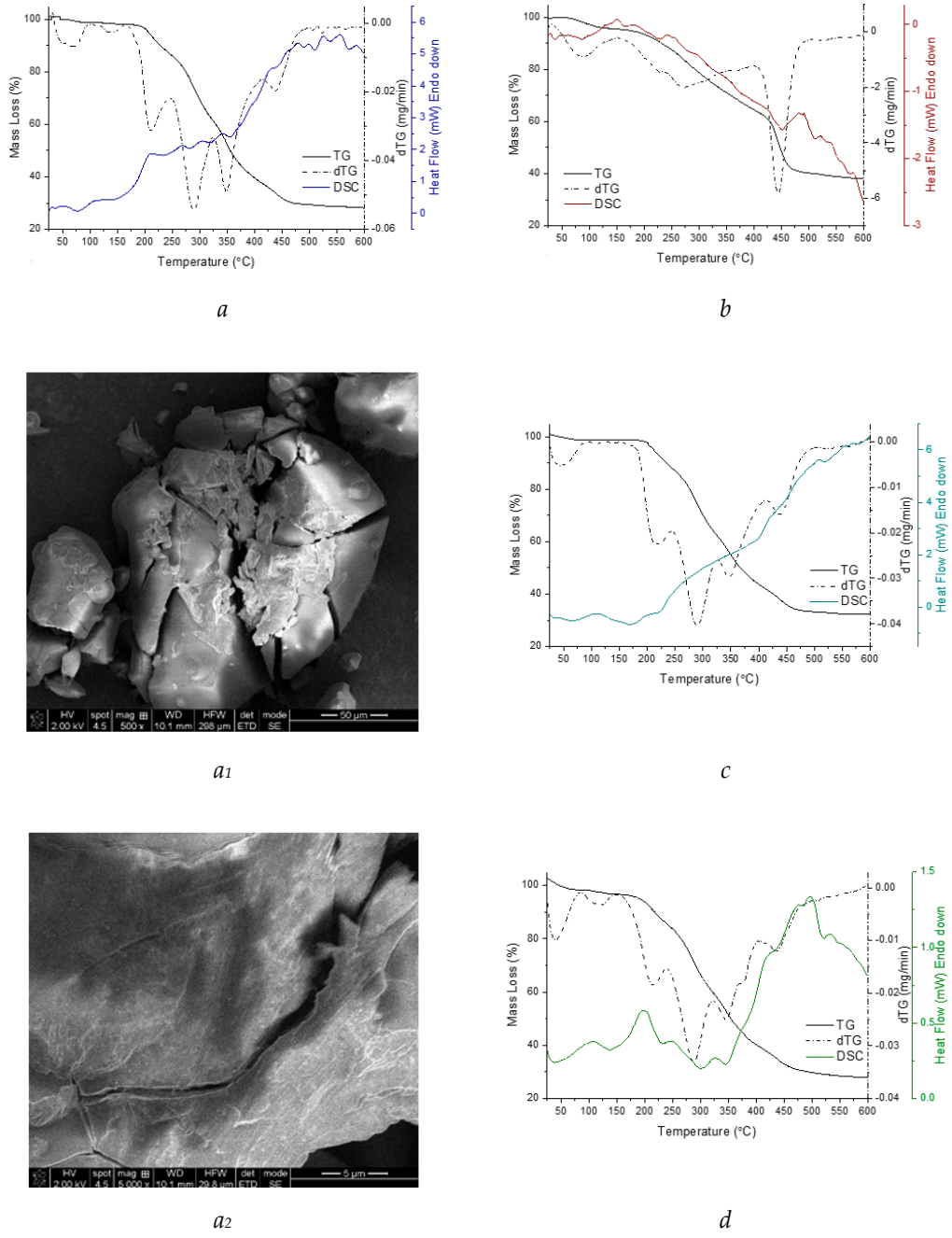

Figure 5. DSC (solid colored line), TG (solid black line), DTG (black dash-dot line) curves of the MC powder resulted from desolvationof MC from acetonitrile – *a*), water – *b*), methanol – *c*) and ethanol – *d*). The pictures (*a*1) (magnification of 500) and (*a*2) (magnification of 5000) represent SEM micrographs of MC powder of sample a), observed at room temperature (25 °C).

Table 4. Thermogravimetric parameters (temperature domain - ΔT and weight loss - Δm) of samples in temperature domain of 25 °C to 600 °C at 10 K/min.

 doi:10.20944/preprints202501.0481.v1

MC(A)		MC(E)		MC(M)		MC(W)	
ΔT[°C]	Δm[%]	ΔT [°C]	Δm [%]	ΔT [°C]	Δm [%]	ΔT [°C]	Δm [%]
25-107.5	2.03	25-164.1	3.56	25-167.8	2.11	25-151.5	4.59
107.5-159.8	0.64	168.1-237.9	10.5	167.8-247.4	11.23	152.6-314.9	19.18
159.8-247.5	11.62	237.9-321.6	25.8	247.4-324.9	25.07	314.9-403.5	12.09
247.5-305.7	19.38	321.6-372.8	14.7	324.7-413.8	20.69	403.5-539.5	24.61
305.7-379.7	23.81	372.8-405.9	6.1	413.8-599.0	9.45	539.5-598.9	1.40
379.7-437.9	9.45	405.9-476.9	8.8				
437.9-599.5	5.52	476.9-599.8	2.67				

The DSC curves of desolvated MC powders are a complex combination of superposed thermal events. It can be seen that there is no distinctly observable phase transitions. The components resulting from the successive degradation (in steps) of the component fragments can be considered as impurities in the remaining sample mass and appear as impurities in the degradation of the following fragments of MC [27] Thus, in the presented thermograms, enlarged endotherms can be observed for the analyzed samples. For such an endotherm, the mathematically calculated peak is very different from the observed peak [28]. MCs samples present a complicated thermal behavior. Therefore, the thermal stability of MC is strongly affected by its molecular conformation and by interactions with the solvent. A perspective is that the MCs samples could be seen as a combination of multiple organic function groups. MC structural function groups could have their own distinct behavior concerning the thermal stability. In MC such function groups may fulfill its own function independently or in cooperation with neighboring functions. Thus, when multiple functional groups are present in a molecule, the individual thermal transitions can overlap or occur at different temperatures, resulting in multiple events on the DSC thermograms [29,30].

Another point of discussion is the polarity of the solvent which contribute to the polymorphic selectivity of MC. This may be possible because at molecular level the solvent selectively absorb onto MC respecting the presence of the function groups present in the molecule [31]. Generally, longer alkyl chains can increase the hydrophobic interactions, leading to increase the melting temperatures [32], but if an electrically charged group is attached to the alkyl group the behavior upon heating will change [33,34]. Thus, the presence of an alkyl sulfate chain linked to an organic structure can affect the melting temperature by influencing the overall molecular structure of MC as well as the interactions within the MC isomer. Moreover, it enhance MC water solubility and affect the stability of merocyanine polymorph in aqueous environments [35,36]. As MC exhibited, a similar thermal behavior has been noted in the literature for ionic liquids, i.e. the melting temperature of ionic liquids with short alkyl chains decreases as the chain length increases [37].In particular, it can be seen in Figure 5a that two solid-solid phase transition are mainly detected in temperature range from 25°C to 100°C.

In the presented thermograms, for MC(A) the endothermic transition at about 37°C is related to the solid-solid polymorphic transition due to the length of the hydrocarbon chain of the butyl sulfonic moiety of MC. This thermal event is followed by another transition almost without loss of mass starting at about 59°C which corresponds to the solid-liquid phase transition of the MC. In the temperature range 150°C to 350°C the curve shows four endotherms for MC(A) due to the thermal transformations of the MC(A) fragments. The components resulting from the mass loss occurs in a wide temperature range and can be clearly observed in Figure 5a) up to around the temperature of 460°C. Table 5 presents the DSC parameters for the thermal events occurring within the temperature range corresponding to the start of heating (25°C) until the modification of the baseline of the thermograms, over which the degradation of the samples occurs through the detachment of component fragments. The thermal events within the considered temperature range correspond to the solid-solid polymorphic transition, the solid-liquid phase transition of the MC, and the release of

 doi:10.20944/preprints202501.0481.v1

remaining solvent molecules, which overlap in this range. It was observed that such degradation temperature is influenced by the solvent that was used in the preparations. Further, a deconvolution of endotherms was done in order to separate the overlapping signals of the MC and solvent located in the same temperature domain. The overlapping transitions of the heating thermograms were deconvoluted into individual constituent peaks (results are in Figure S9 and Table S2) [38]. It was observed that MC desolvates do not have a specific melting point but rather soften over a range of temperatures depending of solvent nature. The results show that the solid-solid transition at about 37°C is clearly evidenced for MC(A) and MC(W), while for MC(M) and MC(E) samples the solvent presence slightly lower the temperature of this transition. For all the samples a stepwise elimination of the solvent took place, possible along with another polymorphic transition. Nevertheless, several aspects as boiling point of the solvents and also their different ability to form physical bonds with function groups of MC must be considered in differentiation of such thermal behavior. In MC(A) and MC(W) samples the solvents ethanol and methanol strongly interact with hydrophobic fragments of MC, resulting in endotherms shifted to higher temperatures in MC(M) and MC(E) samples. Considering the different hydrophobicity and hydrophilicity of the fragments of MC molecule, the obtained results suggest that methanol exhibits a balance between polar and nonpolar characteristics, thus extending the range of interactions of methanol with MC molecule more than the other solvents in this study [39]. However, in the case of the MCW sample, a particularity of the thermal behavior can be highlighted. As can be seen in Figure 5b), the rate of change in mass of sample, as a function of temperature (dTG curves) more clearly reveal the evolution of thermal events. It is observed that the dTG curve of the MCW sample is clearly different from the other samples. Compared to the other samples, MCW shows a significant mass loss (24.61%, as shown in Table 4) at temperature above 400 °C. This suggests that the presence of water has played a role in forming a polymorph with a more thermally resistant arrangement of MC molecules. The FTIR data and the results in Table 2 indicate that the presence of hydrogen bonds leads to stronger interactions between water molecules and MC, which may lead to more pronounced changes in desolvated MC.

Table 5. Thermal paramet ers (the onset- , maximum- , offset- temperatures and corresponding enthalpy) of the main degradation processes of MC polymorphs from DSC data at 10 K/min.

Sample	T_{on} [°C]	T_m [°C]	T_{off} [°C]	ΔH [J/g]
MC(A)	31.08	36.71	49.08	3.25
	51.22	79.30	107.80	30.49
	107.61	113.78	118.80	0.18
	137.36	140.87	150.22	0.70
MC(E)	22.63	38.90	109.94	45.73
	109.53	137.98	163.5	11.38
MC(M)	25.0	30.96	41.77	17.74
	45.86	67.95	96.45	27.98
	149.85	175.19	195.70	37.59
MC(W)	30.83	37.06	43.48	3.48
	68.43	85.77	98.12	6.38
	152.94	163.02	175.31	8.06

In Figure 5, SEM images are shown only for the MCA sample (Figures 5a$_1$,a$_2$) as these were the most appropriate to present. Obtaining the SEM images was challenging due to a number of factors necessary for the accurate recording of the SEM images, which caused real-time modifications of the sample surface. Although we used reasonable recording conditions, consistent with those for sensitive organic substances, parameters such as the chamber pressure (0.08–1.5 Torr) and the energy of the electron beam used for SEM, induced changes to the sample itself (e.g., heating and charging

 doi:10.20944/preprints202501.0481.v1

effects), which to some extent altered the morphology during scan/imaging. However, the SEM instrument we used does not have the capability to capture high-speed events, thus limiting the ability to observe dynamic processes in sensitive samples such as MC desolvates. Nevertheless, we found that MC is highly sensitive to very fine modifications caused by different stimuli, which serves as a premise for future investigations. The fact that MC undergoes phase transitions triggered by various stimuli at physiological temperature (37°C) makes this material ideal for biological applications.

4. Discussion

The solvation of MC involves the interaction between the solvent molecules and its functional groups. Further, the presence of the first solvation sphere, which consists of arrangement the solvent molecules in immediate contact with the MC different function groups can affect the conformation of the MC by stabilizing certain conformations through hydrogen bonding or electrostatic interactions. The solvent polarity and its capability to form hydrogen bonds can influence the conformational preferences of the MC molecule. When the solvent molecules are removed, the intermolecular interactions between the solvent and the MC molecule are disrupted. This can lead to a change in the conformational state of the MC as it seeks to minimize its energy and stabilize itself in the absence of solvent interactions [40,41]. It is important to note that the conformational change resulting from solvent removing is not always predictable and may vary depending on the MC - solvent system. Moreover, Empirical Force Field calculations suggest that solvents influence the conformation of MC molecules by causing the flexible rocking and wagging fragments to fold due to steric hindrance and hydrogen bonding. The interactions between solvent molecules, particularly through hydrogen bonds, constrain the MC molecules, reducing their spatial occupancy. Upon solvent removal, the MC molecules relax into a configuration resembling their solvated state, which in turn shapes the microstructure of the desolvated system.

5. Conclusions

The integration of computational chemistry and physical property experimental evaluation can help to better characterize the merocyanine (MC) conformers of the photoresponsive spirooxazine studied here. In particular, by combining theoretical (MD calculations) and experimental (DSC, TG, SEM, and ATR-FTIR spectroscopy) results, we obtain valuable information about such MC conformers, both in solutions and as a powder. The conformational changes of the MC molecules due to desolvation of their solutions are were specified as based on the impact of the interfacial environment in this case.

The Annealing-MD calculations have shown the structural conformation and interaction of MC molecules with solvents - acetonitrile, ethanol, methanol, and water – as well in their desolvated state. The most stable configurations for both solvated and desolvated MC exhibit preferred orientations of flexible segments, termed "rocking" and "wagging" fragments, which favor the merocyanine isomers with intramolecular hydrogen bond. These fragments adjust their positions to maximize solvent interactions, with the $C_{10}NH_6$ group in MC minimizing contact with OH- groups, influencing the overall molecular packing of MC molecules. In methanol, interactions between MC molecules lead to minimal empty space due to methanol occupying pockets within MC clusters, unlike ethanol and water, which exhibit greater voids within the molecular structures. The simulations indicate that MC's central nitrogen and oxygen atoms can form intra- and intermolecular hydrogen bonds, with the number of these bonds generally increasing upon desolvation, except in methanol. MC exhibits solvatochromism when dissolved in solvents.

The MC polymorphs obtained after desolvationwere characterized experimentally. FT-IR spectral analysis was done for the desolvated MC powders, and their thermal behavior was also discussed. It was established that the polarity of the solvent affects the polymorphic selectivity of MC

 doi:10.20944/preprints202501.0481.v1

by interacting with its functional groups. These interactions influence the thermal stability of MC, which reveals complex thermal events with multiple degradation steps on thermograms.

The findings of the presented study on an MC molecule self-assembly behavior in the presence and absence of various solvents (with properties influenced by the concentration and solvent polarity) indicate a competitive dynamic between intramolecular folding and intermolecular assembly, with the potential for further exploration in the development of advanced functional materials. Knowledge of how MCs solid-state structures are formed and behaved can improve the stability and performance of relevant materials in practical applications.

The information obtained about the stereo-chemical configuration, the flexibility, stability, and other important physicochemical properties of the MC forms of the spirooxazine derivative considered here can be useful for a targeted preparation of such MC conformers from solutions aiming/towards their chemoresponsive functionality. In this case, the specific structure of the solid-phase MC compound that results after the evaporation of the solvent and due to the solvent's influence on the MC molecular arrangement and stability during the transition to a MC solid state, could be very interesting for practical implications and potential applications based on the MC functional groups, orientation of the molecular fragments, molecular shapes and surfaces, molecular packing/clustering, or other possible MC constructs, e.g., composite materials and various kinds of solid (or soft) layers/films. In particular, structures containing MCs are promising to develop chemosensor systems that can be programmed to respond sensitively and specifically to targeted chemical species, such as toxic industrial chemicals, harmful heavy metal ions, or chemical warfare agents. The insights gained from this study may lead to additional innovative materials and applications such as photoactive protective coatings or films with de-manded specific optical and/or barrier properties. Furthermore, MC structures can be used in the development of photocontrollable organic-inorganic hybrid materials with a significant role in nanotechnology.

Supplementary Materials: The following supporting information can be downloaded at the website of this paper posted on Preprints.org.

Author Contributions: For research articles with several authors, a short paragraph specifying their individual contributions must be provided. The following statements should be used “Conceptualization, A.N., V.C., V.A. and S.M.; methodology, A.N., V.C., V.A. and S.M.; validation, A.N., V.C., V.A., G.B.H and S.M.; investigation, A.N., V.C., V.A. and S.M.; resources, A.N. and S.M.; writing—original draft preparation, A.N., V.C. and S.M.; writing—review and editing, A.N., V.C., V.A., G.B.H and S.M.; visualization, A.N., V.C., V.A. and S.M. All authors have read and agreed to the published version of the manuscript.”

Funding: This research received no external funding.

Institutional Review Board Statement: Not applicable.

Informed Consent Statement: Not applicable.

Data Availability Statement: Not applicable.

Acknowledgments: The support of the project “Experimental and Computational Investigations of the Adsorbed Photo-switching Molecules” is acknowledged, through the partners: Institute of Catalysis, Bulgarian Academy of Sciences, Sofia, Bulgaria and Institute of Physical Chemistry of the Romanian Academy, Bucharest, Romania. This research was carried out within the framework of the "Research Innovation and Digitization for Smart Transformation" program 2021-2027 under the Project BG16RFPR002-1.014-0006 "National Centre of Excellence Mechatronics and Clean Technologies" supported by the European Regional Development Fund).

Conflicts of Interest: The authors declare no conflicts of interest.

References

1. Trovato, V.; Sfameni, S.; Rando, G.; Rosace, G.; Libertino, S.; Ferri, A.; Plutino, M.R. A Review of Stimuli-Responsive Smart Materials for Wearable Technology in Healthcare: Retrospective, Perspective, and Prospective. *Molecules* **2022**, *27*, 5709.
2. Sciortino, A.; Marino, E.; Van Dam, B.; Schall, P.; Cannas, M.; Messina, F. Solvatochromism Unravels the Emission Mechanism of Carbon Nanodots. *J. Phys. Chem. Lett*. **2016**, *7*, 3419–3423.

 doi:10.20944/preprints202501.0481.v1

3. Homocianu M. Exploring solvatochromism: A comprehensive analysis of research data. *Microchem. J*. **2024**, *198*, 110166.
4. Karimipour, K.; Keyvan R.J.; Ghomi, A.; Salehi-Mobarakeh, H.; Mahdavian, A. Hydrochromic and photoswitchable polyacrylic nanofibers containing spiropyran in eco-friendly ink-free rewriteable sheets with responsivity to humidity. *Dyes Pigm.* **2020**, *175*, 108185.
5. Martins, C.T.; Lima, M.S.; Seoud, O.A. Thermosolvatochromism of merocyanine polarity indicators in pure and aqueous solvents: relevance of solvent lipophilicity. *J. Org. Chem*. **2006**, *71*, 9068−9079.
6. Fedorov, Y.V.; Shepel, N.E.; Peregudov, A.S.; Fedorova, O.A.; Deligeorgiev, T.; Minkovska, S. Modulation of photochromic properties of spirooxazine bearing sulfobutyl substituent by metal ions. *J. Photochem. Photobiol. A: Chem*. **2019**, *371*, 453−460.
7. Roohi, H.; Rostami, T. Mechanism of the photo triggered ring-opening reaction of spiropyran derivatives (SP-X_{1-7}; X_{1-7} = H, NO_2, CF_3, CN, OH, OMe and NMe_2) in the gas phase and various solvent media: A GD3-TD-DFT approach. *J. Photochem. Photobiol. A: Chem.* **2020**, *392*, 112410.
8. Minkovska, S.; Hadjichristov, G.B.; Neacsu, A.; Chihaia, V.; Fedorov, Y.V. Photoswitchable Photochromic Chelating Spironaphthoxazines: Synthesis, Photophysical Properties, Quantum-Chemical Calculations, and Complexation Ability, *ACS Omega* **2024**, *9*, 4144−4161.
9. Farrell, E.B.; Redmond, G.; Johnson, R.P. Monitoring spirooxazine–merocyanine photoisomerization with ion-current rectifying quartz nanopipettes. *Electrochem. Commun*. **2024**, *168*, 107820.
10. Zeng, W.; Yue, D.; Wang, X.; Li, H.; Kong, X. Synthesis, structural, spectroscopic investigation, Hirshfeld surface analysis and DFT calculation of a new spiro compound including 4-nitroaniline moiety. *J. Mol. Struct.* **2025**, *1322, Part 1*, 140371.
11. Manzoni, V.; Coutinho, K.; Canuto, S. An insightful approach for understanding solvatochromic reversal. *Chem. Phys. Lett*. **2016**, *655-656*, 30–34.
12. Du, D.; Ren, G.-B.; Qi, M.-H.; Li, Z.; Xu, X.-Y. Solvent-Mediated Polymorphic Transformation of Famoxadone from Form II to Form I in Several Mixed Solvent Systems. *Crystals* **2019**, *9*, 161.
13. Jha, K.; Kumar, A.; Munshi, P. Solvatochromism and Reversible Solvent Exchange Phenomena in Solvatomorphic Organic Chromophore Crystals, *Cryst. Growth Des*. **2023**, *23*, 2922–2931
14. Sun, H. COMPASS: An ab Initio Forcefield Optimized for Condensed-Phase Applications - Overview with Details on Alkane and Benzene Compounds. *J. Phys. Chem. B* **1998**, *102*, 7338−7364.
15. Thompson, A.P.; Aktulga, H.M; Berger, R.; Bolintineanu, D.S.; Brown, W.M.; Crozier, P.S.; in 't Veld, P. J.; Kohlmeyer, A.; Moore, S.G.; Nguyen, T.D.; Shan, R.; Stevens, M.J.; Tranchida, J.; Trott, C.; Plimpton, S.J. LAMMPS - a flexible simulation tool for parti-cle-based materials modeling at the atomic, meso, and continuum scales. *Comp. Phys. Comm*. **2022**, *271*, 10817.
16. Robinson, R.L.M.; Geatches, D.; Morris, C.; Mackenzie, R.; Maloney, A.G.P.; Roberts, K.J.; Moldovan, A.; Chow, E.; Pencheva, K.; Vatvani, D.R.M. Evaluation of Force-Field Calculations of Lattice Energies on a Large Public Dataset, Assessment of Pharmaceutical Relevance, and Comparison to Density Functional Theory. *J. Chem. Inf. Model*. **2019**, *59*, 4778−4792.
17. Jmol: an open-source Java viewer for chemical structures in 3D. http://www.jmol.org/
18. Neese F.; Software update: The ORCA program system—Version 5.0. *WIREs Comput. Molec. Sci.*, **2022**; *12*, e1606. Neese, F.; Wennmohs, F.; Becker, U.; Riplinger, C. The ORCA quantum chemistry program package. *J. Chem. Phys.* **2020**, *152*, 224108.
19. Becke, A. D. Density-functional thermochemistry. III. The role of exact exchange. J. Chem. Phys. 1993, 98, 5648−5652.
20. Rassolov, V. A.; Pople, J. A.; Ratner, M. A.; Windus, T. L. 6-31G* basis set for atoms K through Zn. J. Chem. Phys. 1998, 109, 1223−1229.
21. Nordin, R.; Lazim, A.M.; Rohadi, A.; Hasbullah, S.A. Preparation and Activation of Spiropyran-Merocyanine System. *Malay. J. Anal. Sci.* **2013**, *17*, 422–429.
22. Todorova, M.; Bakalska. R. Syntheses and vibrational spectroscopic characteristics of series ionic merocyanine dyes. *Bulg. Chem. Commun*. **2018**, *50*, 156−164.

 doi:10.20944/preprints202501.0481.v1

23. Gegiou, D.; Lambi, E.; Hadjoudis, E. Solvatochromism in N-(2-Hydroxybenzylidene)aniline, N-(2-Hydroxybenzylidene)benzylamine, and N-(2-Hydroxybenzylidene)-2-phenylethylamine. *J. Phys. Chem*. **1996**, *100*, 17762−17765.
24. Basu, K.; Brielle, E.S.; Arkin, I.T. Hydrogen Bond Strengthens Acceptor Group: The Curious Case of the C–H···O=C Bond. *Int. J. Mol. Sci*. **2024**, *25*, 8606.
25. Bartlett, G.J.; Newberry, R.W.; VanVeller, B.; Raines, R.T.; Woolfson, D.N. Interplay of hydrogen bonds and n→π* interactions in proteins. *J. Am. Chem Soc.* **2013**, *135*, 18682-18688.
26. Arnaudov, M.G. The influence of the medium on the infrared spectrum of self-associated systems. A structural analysis. *Int. J. Vib. Spectrosc.* **2001**, *5*, 5.
27. Rojek, B.; Bartyzel, A.; Sawicki, W.; Plenis, A. DSC, TGA-FTIR and FTIR Assisted by Chemometric Factor Analysis and PXRD, in Assessing the Incompatibility of the Antiviral Drug Arbidol Hydrochloride with Pharmaceutical Excipients. *Molecules* **2024,** *29*, 264.
28. Gill, P.; Moghadam, T.T.; Ranjbar, B. Differential scanning calorimetry techniques: applications in biology and nanoscience. *J. Biomol. Tech*. **2010**, *21*, 167-93
29. Leyva-Porras, C.; Cruz-Alcantar, P.; Espinosa-Solís, V.; Martínez-Guerra, E.; Piñón-Balderrama, C.I.; Martínez, I.C.; Saavedra-Leos, M.Z. Application of Differential Scanning Calorimetry (DSC) and Modulated Differential Scanning Calorimetry (MDSC) in Food and Drug Industries. *Polymers* **2020**, *12*, 5.
30. Arneri, G.; Sauer, J.A. Study of overlapping transitions in polymers by combined differential scanning calorimetry and thermal optical analysis methods. *Thermochim. Acta* **1976**, *15*, 29−41.
31. Mudalip, S.K.A.; Bakar, M.R.A.; Jamal, P.; Adam, F.; Man, R.C.; Sulaiman, S.Z.; Arshad, Z.I.M.; Shaarani, S.M. Effects of Solvents on Polymorphism and Shape of Mefenamic Acid Crystals. *Proc. MATEC Web Conf. (MUCET2017)* **2018**, *150*, 02004.
32. Villanueva, M.; Vallet, P.; Teijeira, T. Santiago A.A.; Amigo, A.; Tojo, E.; Varela, L.; Parajó, J.; Salgado, J. Effect of alkyl chain length on the thermal properties and toxicity of n-alkyl-ammonium nitrate ionic liquids (n = 2, 3, 4, 5, 6, 8) for energy applications. *J. Therm. Anal. Calorim.* **2024**, https://doi.org/10.1007/s10973-024-13333-y.
33. Jeong, E.; Ito, T; Takahashi, K.; Koganezawa, T.; Hayashi, H.; Aratani, N.; Suzuki, M.; Yamada, H. Exploration of Alkyl Group Effects on the Molecular Packing of 5,15-Disubstituted Tetrabenzoporphyrins toward Efficient Charge-Carrier Transport. *ACS Appl. Mater. Interfaces* **2022**, *14*, 32319−32329
34. Sai, R.; Hirata, S.; Tsutsumi, H.; Katayama, Y. Effect of Alkyl Side Chain Length on the Lithium-Ion Conductivity for Polyether Electrolytes. *Front Chem*. **2022**, *14*, 943224.
35. Kulinich, A V; Ishchenko, A. Merocyanine dyes: synthesis, structure, properties and applications. *Russ. Chem. Rev*. **2009**, *78*, 141–164.
36. Abeyrathna, N.; Liao, Yi. Stability of merocyanine-type photoacids in aqueous solutions. *J. Phys. Org. Chem.* **2017**, *30*, e3664.
37. Zhang, Y.; Maginn, E.J. Molecular dynamics study of the effect of alkyl chain length on melting points of [C_nMIM][PF_6] ionic liquids. *Phys. Chem. Chem. Phys*. **2014**, *16*, 13489−13499.
38. The peaks deconvolution was done by OriginPro 9.0.0, OriginLab Corporation, Massachusetts, USA https://www.originlab.com
39. Kvamme, B.; Wei, N.; Zhao, J.; Zhou, S.; Zhang, L.; Sun, W.; Saeidi, N. Alcohols for hydrate inhibition - Different alcohols and different mechanisms. *Petroleum* **2022**, *8*, 1-16.
40. Xin, L.; Wang, N.; Jinyue, Y.; Huang, Y.; Ji, X.; Huang, X.; Wang, T.; Wang, H.; Hao, H. Molecular conformational evolution mechanism during nucleation of crystals in solution. *IUCrJ*. **2020**, *7*, 542−556.
41. Hernández-Lima J.; Ramírez-Gualito K.; Quiroz-García B.; Silva-Portillo A.L.; Carrillo-Nava E.; Cortés-Guzmán F. How solvent determines the molecular reactive conformation and the selectivity: Solvation spheres and energy. *Front. Chem*. **2022**, *10*, 1012769.